The 11th International Topical Meeting on Nuclear Reactor Thermal-Hydraulics (NURETH-11)
Popes Palace Conference Center, Avignon, France, October 2-6, 2005.

Log Number: 492

NUMERICAL INVESTIGATION OF THE LEAKAGE BEHAVIOUR OF REINFORCED CONCRETE WALLS

Christoph Niklasch[1], Institut für Massivbau, Universität Karlsruhe (TH), Germany
Phone: +49 721 608 4352, Fax: +49 721 608 2265, christoph.niklasch@ifmb.uni-karlsruhe.de

Laurent Coudert, Gregory Heinfling, Chantal Hervouet, Benoît Masson
EDF, France

Nico Herrmann, Lothar Stempniewski
Institut für Massivbau, Universität Karlsruhe (TH), Germany

ABSTRACT

For the verification of nuclear power plant safety, the leakage behaviour of the containment walls is of decisive importance. Extreme temperatures well over the water boiling temperature accompanied by high internal pressures can occur during an severe accident. In case of cracks through the entire thickness of the containment wall, an air-steam-water mixture may be released.
In order to improve the knowledge of the leakage behaviour through cracks during such abnormal occurrences an experimental setup was developed at IfMB and several tests with different parameters were performed. The details of the experimental facility and the performed tests will be described in a separate paper.
To improve the understanding of the behaviour of the tested wall elements during the tests numerical simulations of the performed leakage experiments are necessary. Reliable numerical tools provide a basis for the transfer of the leakage behaviour from the tested specimens to the behaviour of whole containment structures. To address the task of developing tools for the numerical simulation of the leakage behaviour of reinforced containment structures, EDF and IfMB decided to cooperate.
During this cooperation two different numerical approaches had been made basing on existing tools and models of EDF and IfMB. In the following sections a short overview about the two different models will be given.
For the numerical investigation of the leakage phenomena IfMB used the commercial Finite-Element-Program ADINA with ADINA's capability to solve coupled fluid-structure-interaction (FSI) problems. For the investigation of the moving of the specimen and the change of the crack profiles during the tests, it is important to take into account the heating of the specimen by the fluid flowing through the cracks.
This is done by an iterative calculation of the fluid model and the structural model of the specimen. The thermo-dynamic boundary conditions representing the behaviour inside the pressure chamber with pressure, temperature and air-steam ratio according to the scenario of the experiments and the convection boundary conditions representing the environmental conditions outside the specimen are defined for the fluid model. The heat capacity and thermal conductivity are chosen according to values determined at concrete samples of the tested specimen. For the fluid a special model was added to ADINA in order to simulate the air/steam/water flow inside the cracks.
The structure of the specimen is modelled as a two-dimensional model. For the modelling of the concrete parts of the specimen a concrete material model developed at IfMB was used. The concrete elements were linked to the reinforcement with bond elements to simulate the load introduction from the reinforcement into the concrete and to allow relative displacements between reinforcement and concrete. The calculated displacements and crack profiles of the solid model were used as input parameters for the next iteration step of the fluid model.

[1] Corresponding author

Investigation of the leakage behaviour of reinforced concrete walls

Nico Herrmann, Christoph Niklasch, Michael Stegemann, Lothar Stempniewski
Institute of Reinforced Concrete Structures and Building Materials
University of Karlsruhe, Germany

1 Introduction

Information about the leakage behaviour of the containment in case of an accident is of decisive importance for the verification of nuclear power plant safety. Assuming a core melt accident with failure of the reactor vessel in a pressurized water reactor, high internal pressures accompanied by temperatures well over the water boiling temperature can occur. During loss of the primary coolant a large quantity of steam develops. In case of resulting cracks through the entire thickness of a pre-stressed containment wall without liner, an air-steam mixture enriched with aerosols may be released.

Regarding the leakage of pure air through cracked concrete walls there are a couple of investigations introducing correlations based on crack width and pressure differential, like [7], [12] for instance. The leakage behaviour of water through cracked concrete walls has already been investigated as well [3], [9]. Investigations on the leakage of steam and air through narrow, idealized cracks were performed in [1]. However, corresponding knowledge about the leakage of air-steam mixtures through real cracks was missing world-wide so far.

2 Conception of the experiments

The leakage observation can be divided in mechanical processes determining cracks through the wall and the thermo-hydraulic processes. The development of crack patterns and average crack widths can be calculated quite well using available numerical procedures like the finite element method [5]. Contrary to the mechanical processes it's difficult to describe the parameters governing the thermo-hydraulic processes inside the cracks like roughness, temperature, heat transfer and condensation.

Part of the project was to analyse the thermo-hydraulic process of water-air exchange with condensation through known crack patterns. In contrast to other investigations on large scale model containments, see MAEVA [5], it was not intended to simulate the integral behaviour of the containment as a whole but of a representative section of the containment wall.

Integral tests were performed on specially developed specimens with complex and realistic crack patterns. Due to the applied axial load during cracking the induced cracks are of almost uniform mean widths. The thermo-hydraulic load used for the tests followed a severe accidental scenario based on the design scenario for a core melting accident of the EPR (Fig. 1).

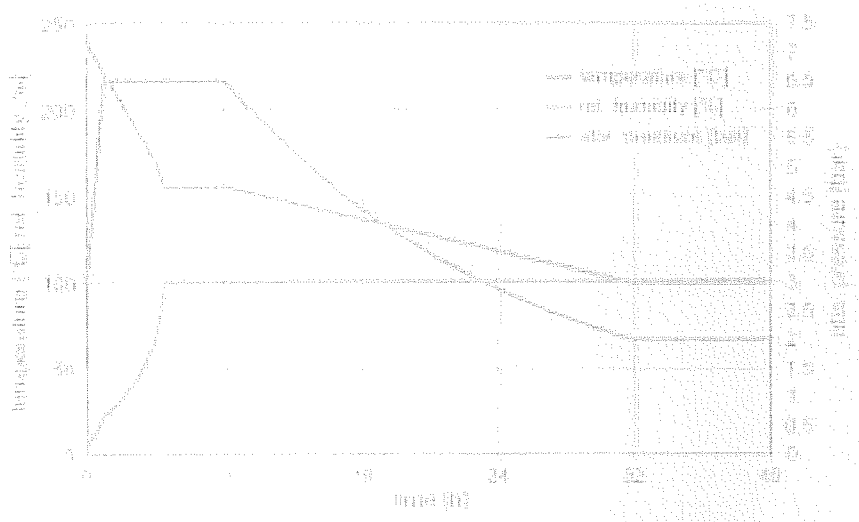

Fig. 1: Test scenario

3 Testing facility

3.1 Mechanical set-up

The mechanical part of the testing facility consists of a load frame, two abutments, 12 hydraulic jacks, a pressure chamber above the specimen and a control room underneath. The mechanical set-up is shown in Fig. 2 and Fig. 3. The abutment for the anchorage and the abutment for the hydraulic jacks are connected together with the load frame and form a closed load path between the jacks and the abutments.

Additionally the load frame rests, through the reinforced concrete cover of the pressure chamber and sealing, on an abutment for pressure cushions sealing the cracks at the side of the specimen. Above the specimen is a steel made insulated pressure chamber, fixed by a reinforced concrete cover and bolted down to the load frame. The pressure chamber has an area of 3.25 m² and a volume of about 1 m³. The air-steam-mixture enters the pressure chamber at one side. After leaking through the specimen the outflow of condensed water and air is trapped in a control room. The amount of leakage is measured after the control room.

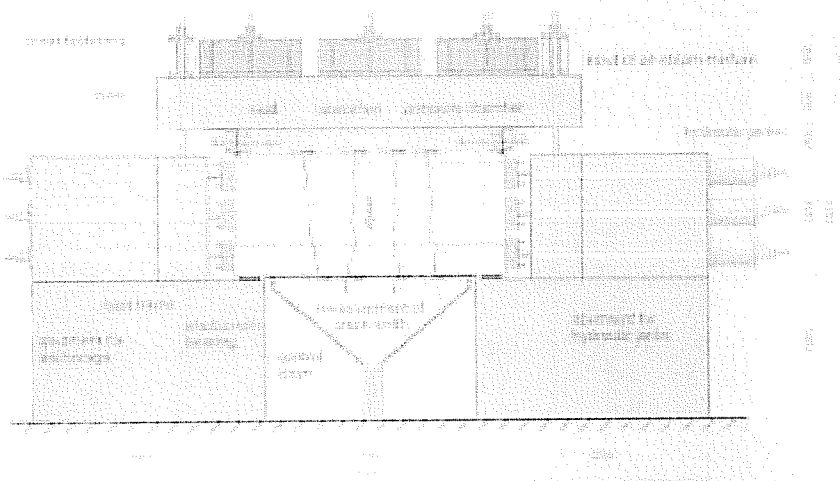

Fig. 2: Vertical cross section

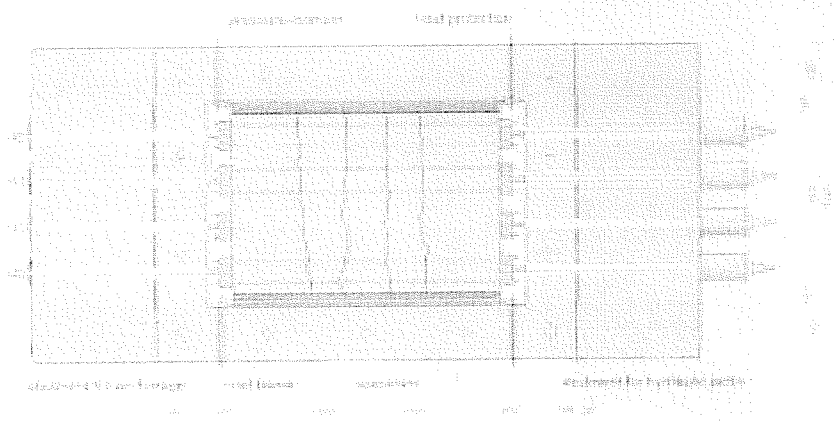

Fig. 3: Horizontal cross section

In order to ensure the desired pressure, temperature and humidity conditions and to avoid unwanted condensation, a minimum flow through the pressure chamber is established by opening an additional bypass valve opposite the mixture inlet.

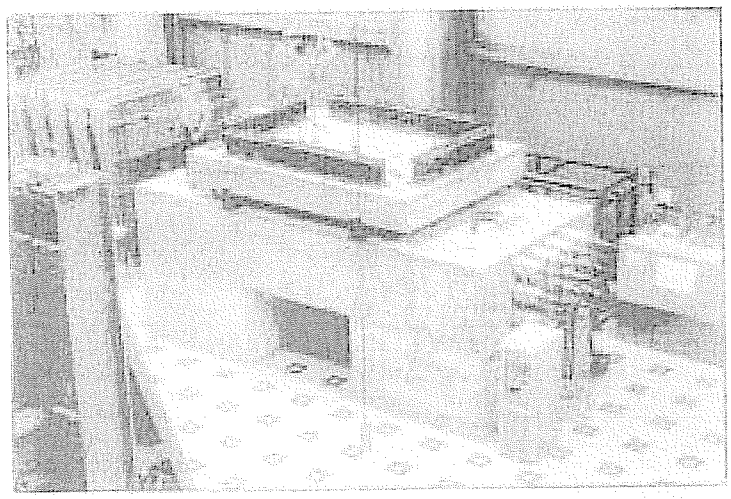

Fig. 4: Total view of the testing facility

3.2 Thermo-hydraulic set-up

Aim of the design process of the thermo-hydraulic set-up was to achieve stable air-steam mixtures matching complex, highly time dependent accidental scenarios. To fulfil the predefined accidental scenarios it is necessary to regulate the parameters temperature, partial pressure of steam and partial pressure of air. These three parameters describe the physical state completely at any time. The production principle of the air-steam-mixture is shown in Fig. 5. Unlike temperature, the parameters partial pressure air and partial pressure steam are not available for directly measurement. It is necessary to define the system state in equivalent measurable parameters. Instead of the partial pressures the total pressure and the relative humidity are measured and taken as a control parameters.

The main parts of the air steam mixture process are the compressor, boiler, static mixer, air heater, steam super-heater and 3 pneumatic valves.

The generator can be inverted in the air channel, the steam channel and the air-steam-mixture channel on the inlet side of the specimen, a bypass channel on the outlet side and the control room to collect leakage. The measurement and control system of the mixture production is realized using five control loops for temperature, pressure, relative humidity and mixture flow.

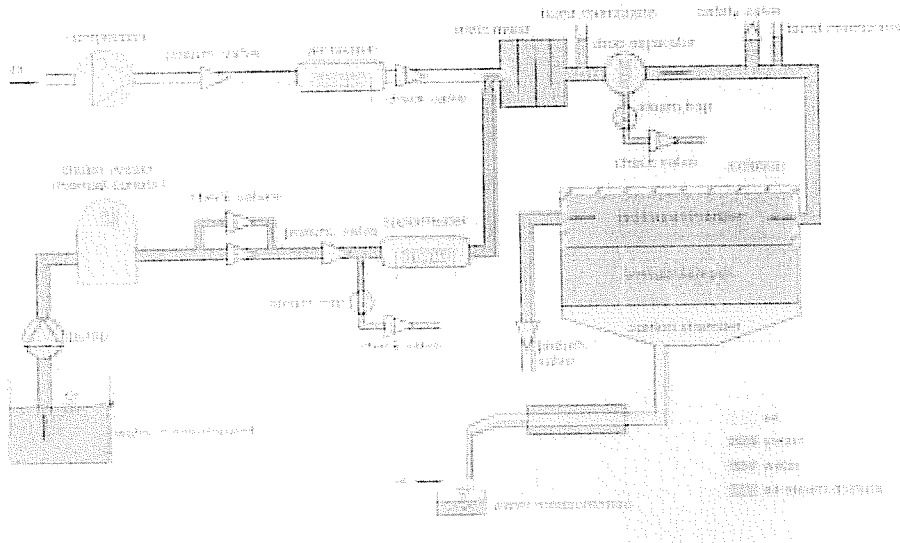

Fig. 5: Air-steam-mixture generation principle

Temperature	100..152 °C	saturated steam-air mixtures
	100..250 °C	superheated steam-air mixtures
	20..250 °C	pure air
pressure	1..6.5 bar absolute	
relative humidity	1..100 %	
max. steam capacity	500 kg/h	

Tab. 1: Capabilities of the air-steam-mixture process

3.3 Specimen

Two specimen are reinforced concrete slabs with dimensions of 2.7 m x 1.8 m x 1.2 m. These dimensions are based on the following boundary conditions:

- Thickness of 1.2 m is equivalent to the design wall thickness of EPR
- The maximum force available for axial tensile cracking of the specimen limits the cross section area and determined the width to 1.8 m
- To achieve an observation area of 1.8m x 2.0m a total specimen length of 2.7m is needed to allow load introduction being completed outside the observation area

Two different types of specimen with same overall dimensions have been developed. The first type has only longitudinal reinforcement. This allows a free development of the crack pattern along cross section. The reinforcement layout is shown in Fig. 6.

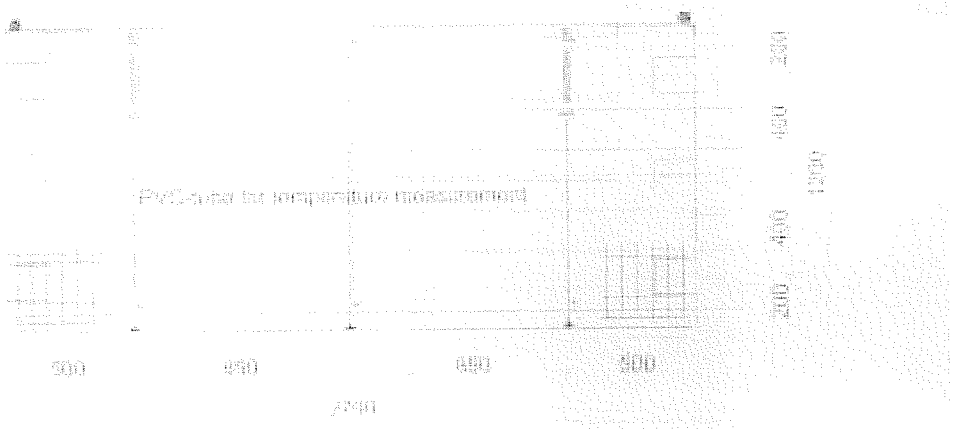

Fig. 6: Vertical section specimen type 1

The second specimen type is enveloped with ducts and a surface mesh reinforcement equivalent to the EPR containment design. Fig. 7 shows a longitudinal section through the second specimen type with 2 layers of longitudinal ducts on the external side and one layer of transversal ducts above. A reinforcement mesh is located near both surfaces for crack distribution.

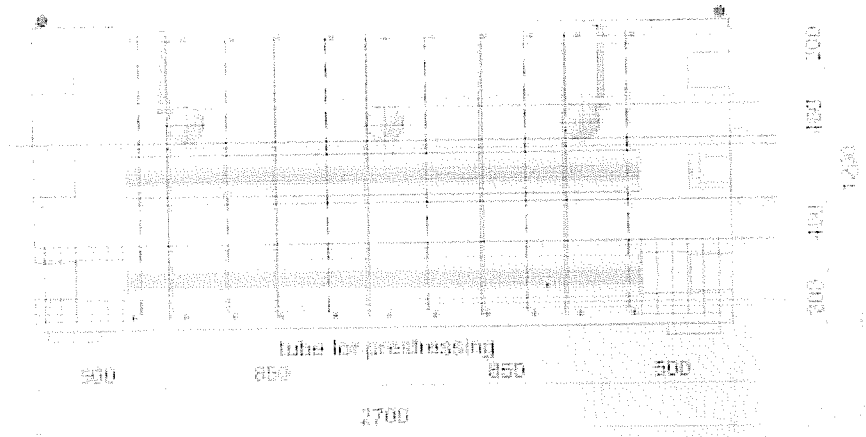

Fig. 7: Vertical section specimen type 2

The longitudinal reinforcement bars of both specimen types are used only for load introduction. The cracks are induced by applying axial tension with the hydraulic jacks. During the tests the external crack width is adjusted by changing the applied load of the jacks and can be modified independent from the pressure inside the pressure chamber.

4 Results

So far, two type 1 specimens and one type 2 specimen have been produced and tested. The first specimen served only to calibrate the air-steam-mixture process.

number of experiment	crack length [mm]	mean crack width at external side [mm]	crack width during experiment [mm]		total leakage [liter/h/0]
			external side top (max)	external side, bottom (max)	
VK310	ca. 3,45	"0"	0,007	0,07	0,195
VK312	ca. 3,45	0,15	0,007	const. 0,15	~ 200
VK311	ca. 3,75	"0"	0,005	0,07	1,3
VK313	ca. 3,75	0,35	0,11	const. 0,35	~ 440

Tab. 2: Overview of the performed experiments

4.1 Preparation of specimen 2

The second specimen is described for relevance of the established testing procedure. It is a type 2 specimen with ducts and a surface mesh reinforcement.

The cracks were induced 139 days after casting applying a maximum axial force with the hydraulic jacks of 7000 kN. The crack pattern obtained is shown in Fig. 8.

Displacement transducers were mounted after crack induction onto the top and the bottom surfaces in order to measure the crack widths during the thermo-hydraulic scenario. If the crack width on the external side varied, it was adjusted by changing the load applied by the hydraulic jacks.

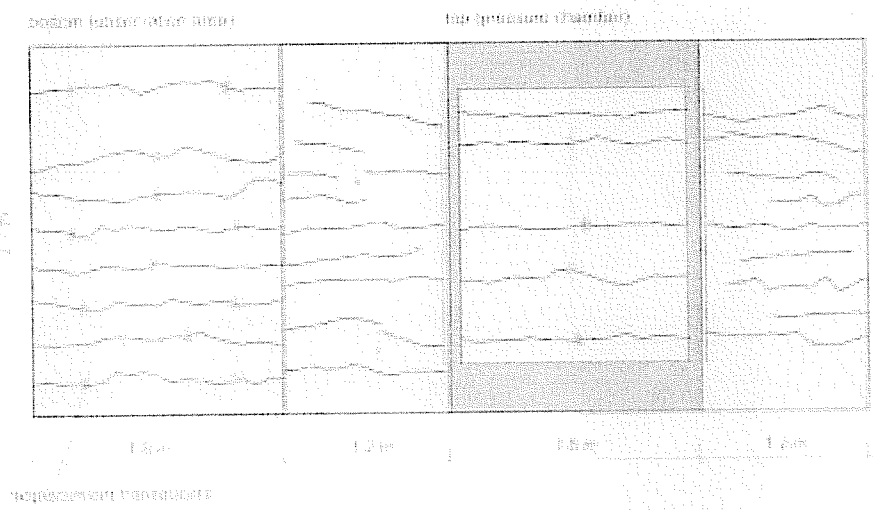

Fig. 8: Crack pattern of specimen 2

4.2 Tests with specimen 2

The first steam test VK2/1 was performed with closed cracks without axial load in order to simulate a cracked wall with remaining crack widths only. During the test with closed cracks there was hardly any leakage.

For the second steam test VK2/2 the average crack width was adjusted to 0,15 mm. The crack width at the bottom surface was kept constant during the whole 40 hour scenario by changing the applied axial load. The crack width change at the top surface side of the specimen followed the temperature inside the pressure chamber (Fig. 9).

The measured leakage rate is shown in Fig. 10. For a better comparability the leakage is based on a unit crack length of 1 m, a pressure of 1 bar and a temperature of 0 °C. The steam condensed entirely inside the cracks and no steam outflow was observed. The total amount of leakage during the whole 40 hour scenario was about 200 l of water.

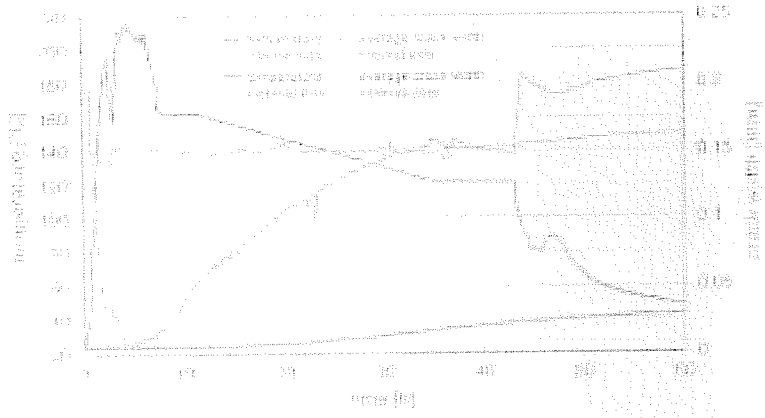

Fig. 9: Temperature and crack width specimen 2/2

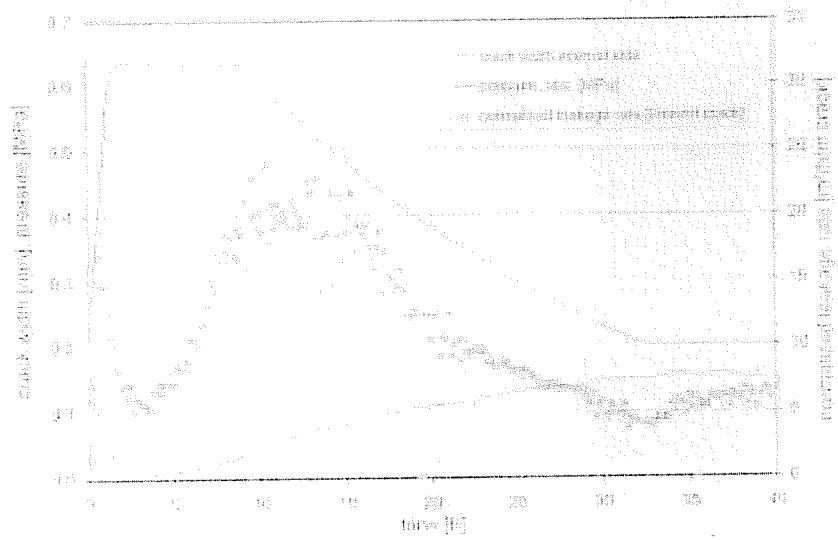

Fig. 10: Leakage of specimen 2/2

5 Conclusions

In the total 30 leak tests were performed with 7 different pre-cracked specimen types. During tests with closed cracks no measurable leakage was found. During tests with average crack widths of 0.15 mm and 0.30 mm water outflow was observed only. The steam condensed entirely inside the specimen. The test results can be used for a first estimation of the integral containment-leakage behaviour for a given crack pattern.

6 Literatur

[1] Carol, C.; Coulon, N.; Morton, D.A.V.; Williams, M.M.R.: *Theoretical and Experimental Investigations on the Leakage of Steam, Gas and Aerosols through narrow Cracks and Capillaries*, Symposium on EU Research on Severe Accidents, Luxembourg, 1995

[2] Danisch, R.; Huby, Y.: *Containment design of the European Pressurized Water Reactor (EPR)*, Vortrag ANS-Meeting, Orlando, 1997

[3] Edvardsen, C.K.: *Wasserundurchlässigkeit und Selbstheilung von Trennrissen im Beton*, DAfStb Heft 455, Beuth, Berlin 1996

[4] Eibl, J.: *Zur dauerhaften Abdichtung eines alternativen Containments für Druckwasserreaktoren*, Bericht KfK 5366, Kernforschungszentrum Karlsruhe, 1994

[5] Eibl, J.; Bunler, A.: *Grenztragfähigkeit von Stahlbetonumschließungen im Kernkraftwerksbau*, Teilbericht 2b: Selbstentlastung, Schlussbericht zum Forschungsvorhaben BMU SR 413

[6] Eibl, J.; Ramm, W.; Tolleer, M.; Abbelmann, J.; Hartmann, N.; Reitze, R.; Elz, S.: *Investigations of the leakage behaviour of reinforced concrete walls*, Schlussbericht zum Forschungsvorhaben BMWi 150 1053, 2001

[7] Gremer, U.; Rostam, W.: *Air leakage characteristics in cracked concrete*, Nuclear Engineering and Design, Vol. 156, 1995

[8] Guinot, P.; Devaliu, A.; Lancia, B.; Barre, F.: *Design and erection of a large mock-up of containment under severe accidental conditions*, Trans. 14th Int. Conf. Struc. Mech. in Reactor Techn. (SMIRT-14), Lyon, France, 1997

[9] Imbol-Zeller, C.: *Fließverhalten von Flüssigkeiten in durchgehend gerissenen Betonkonstruktionen*, DAfStb Heft 460, Beuth, Berlin, 1996

[10] König, G.; Fehling, E.: *Zur Rissbreitenbeschränkung im Stahlbetonbau*, Beton- und Stahlbetonbau 6/1988, 161-167

[11] König, G.; Tue, N.V.: *Grundlagen und Bemessungshilfen für die Rissbreitenbeschränkung im Stahlbeton und Spannbeton*, DAfStb Heft 466, Beuth, Berlin 1996

[12] Rizkalla, S.H.; Assur, M.; Lau, B.T.; Simmonds, S.H.: *Air Leakage Characteristics in Reinforced Concrete*, Journal of Structural Engineering, Vol. 110, No. 5, May 1984

NUMERICAL INVESTIGATION OF THE LEAKAGE BEHAVIOUR OF REINFORCED CONCRETE WALLS

Christoph Niklasch[1], Institut für Massivbau (IfMB), Universität Karlsruhe (TH), Germany
Laurent Coudert, Gregory Heinfling, Chantal Hervouet, Benoît Masson, EDF, France
Nico Herrmann, Lothar Stempniewski, Universität Karlsruhe (TH), Germany
Phone: +49 721 608 4352, Fax: +49 721 608 2265, christoph.niklasch@ifmb.uni-karlsruhe.de

ABSTRACT

For the verification of nuclear power plant safety, the leakage behaviour of the containment walls is of decisive importance. In order to improve the knowledge of the leakage behaviour through cracks during a severe accident an experimental setup was developed at IfMB and several tests with different parameters were performed. To improve the understanding of the behaviour of the wall elements during the tests numerical simulations of the performed leakage experiments are necessary. Reliable numerical tools provide a basis for the transfer of the leakage behaviour from the tested specimens to the behaviour of whole containment structures. To address the task of developing tools for the numerical simulation of the leakage behaviour of reinforced containment structures, EDF and IfMB decided to cooperate. During this cooperation two different numerical approaches had been made basing on existing tools and models of EDF and IfMB. In the following sections a short overview about the two different models will be given. For the numerical investigation of the leakage phenomena IfMB used the commercial Finite-Element-Program ADINA with its capability to solve coupled fluid-structure-interaction (FSI) problems. EDF used two of their self-developed tools for the numerical simulation in a chained calculation: CODE ASTER® for the mechanical calculation of the specimen and ECREVISSE for the air/steam/water leakage flow calculation. The calculated leakage rates and temperature profiles of both models will be compared to the experimentally determined leakage rates and the results will be discussed.

KEYWORDS

containment, leakage behaviour

1 INTRODUCTION

During severe accidents in nuclear power plants high internal pressures accompanied by temperatures well over the water boiling temperature can occur and an air-steam mixture may be released through cracked containment walls.

Regarding the leakage of pure air through cracked concrete walls there are a couple of investigations introducing correlations based on crack width and pressure differential, like (Greiner & Ramm, 1995), or (Rizkalla *et al.* , 1984). The leakage behaviour of water through cracked concrete walls has already been investigated as well by Edvardsen (1996) and Imhof-Zeitler (1993). Investigations on the leakage of steam and air through narrow, idealized cracks were performed in (Caroli *et al.* , 1995).

To improve the knowledge about the leakage behaviour of reinforced concrete walls a test set-up was developed at the Institute of Reinforced Concrete Structures and Building Materials at the Universität Karlsruhe (TH). The results of the first series of tests were published by Herrmann *et al.* (2002).

In this paper the results of the first test performed for EDF with an improved set-up and a new scenario will be presented. In the second part of the paper, numerical simulations of the test performed

[1]Corresponding author

by IfMB and EDF will be presented and compared with the experimental results. More test results will be published by Stegemann (2005).

2 TESTING FACILITY

2.1 Mechanical set-up

The mechanical part of the testing facility consists of a load frame, two abutments, 12 hydraulic jacks, a pressure chamber above the specimen and a control room underneath. The mechanical set-up is shown in Figure 1 and Figure 2. The abutment for the anchorage and the abutment for the hydraulic jacks are connected together with the load frame and form a closed load path between the jacks and the abutments. Additionally the load frame holds down the reinforced concrete cover of the pressure chamber and works as an abutment for pressure cushions sealing the cracks at the side of the specimen. Above the specimen is a steel made insulated pressure chamber, fixed by a reinforced concrete cover and bolted down to the load frame. The pressure chamber has an area of 3.28 m^2 and a volume of about 1 m^3. The air-steam-mixture enters the pressure chamber at one side. After leaking through the specimen the outflow of condensed water and air is trapped in a control room. The leakage is devided into condensed water and air and measured seperatly after the control chamber. In order to ensure the desired pressure, temperature and humidity conditions and to avoid unwanted condensation, a minimum flow through the pressure chamber is established by opening an additional bypass valve opposite to the mixture inlet.

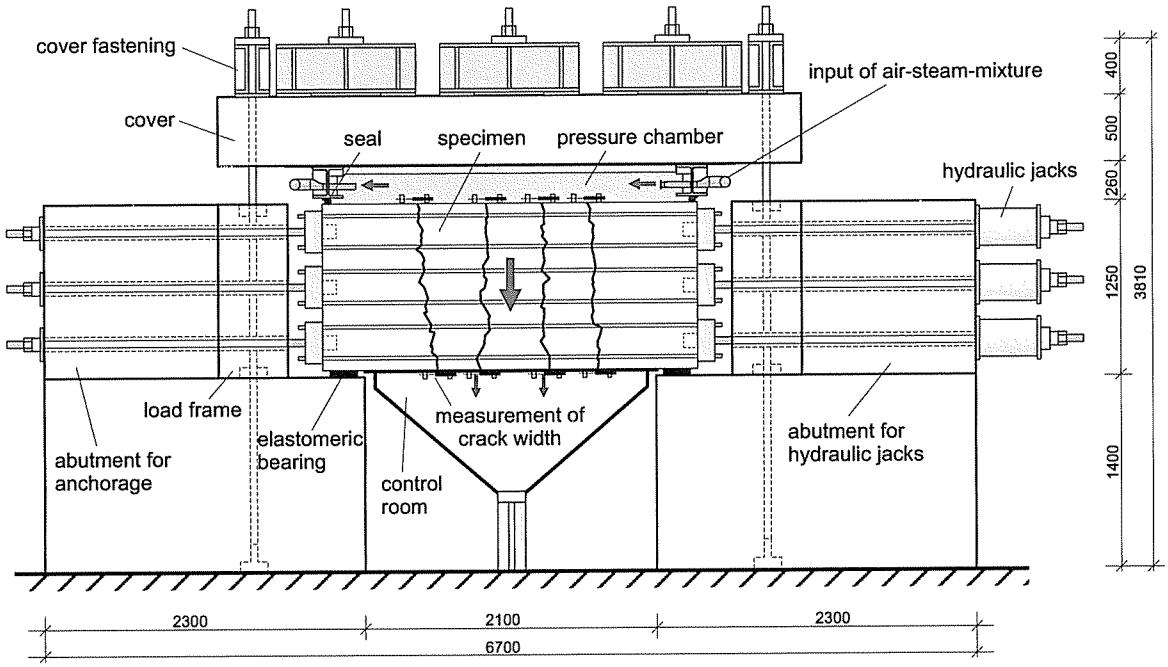

Figure 1: Vertical cross section

2.2 Specimen

The specimen are reinforced concrete slabs with dimensions of 2,7 m x 1,8 m x 1,2 m and only longitudinal reinforcement. The reinforcement layout is shown in figure 3. To allow a free development of the crack pattern, no crack-inducing parts are embedded. The necessary tensile stresses for the cracking are introduced with the 12 hydraulic jacks into the longitudinal reinforcement bars and with the bond between reinforcement and concrete into the concrete. The number of the cracks and the minimal spacing between the cracks therefore depends on the bond behaviour between concrete and reinforcement.

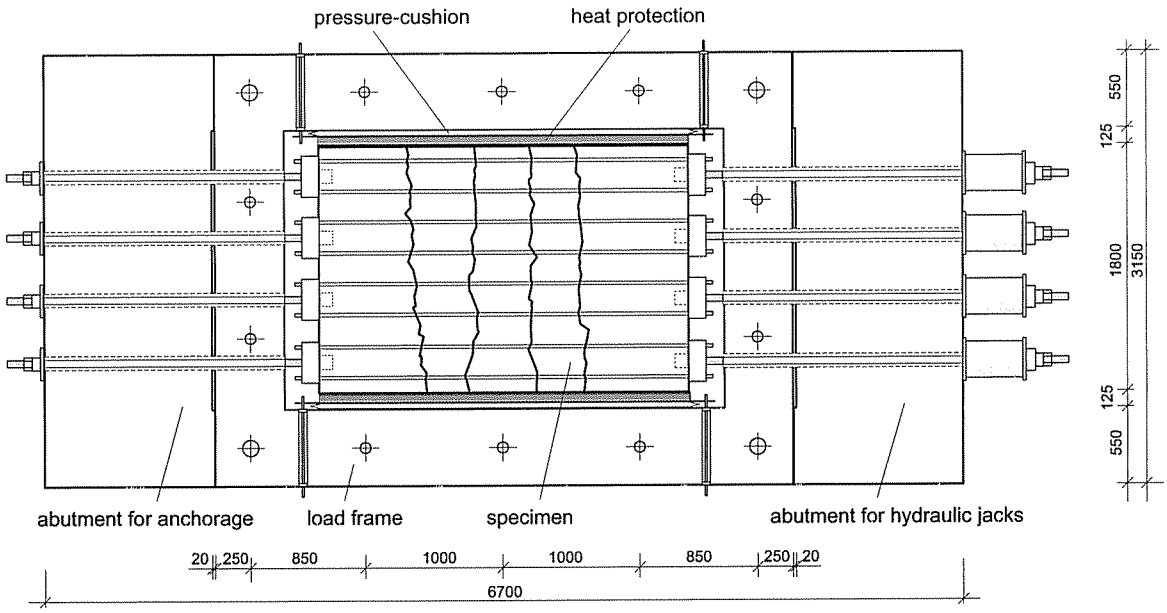

Figure 2: Horizontal cross section

2.3 Thermo-hydraulic set-up

The aim of the design process of the thermo-hydraulic set-up was to achieve stable air-steam conditions matching complex, highly time dependent scenarios. To fulfil the predefined scenarios it is necessary to regulate the pressure, the ratio of steam and air and the temperature of the mixture. These three parameters describe the physical state completely at any time. The main parts of the machine are the steam boiler, the compressor, the static mixer, air heater, steam super-heater and 3 pneumatic valves. More details on the thermo-hydraulic set-up can be found in (Herrmann *et al.* , 2002) and (Stegemann, 2005).

2.4 Steam test procedure Specimen One

A crack pattern with 5 cut-through cracks was induced with the 12 hydraulic jacks before the steam test. After unloading of the specumen an average crack width of 0.07 μm remained.

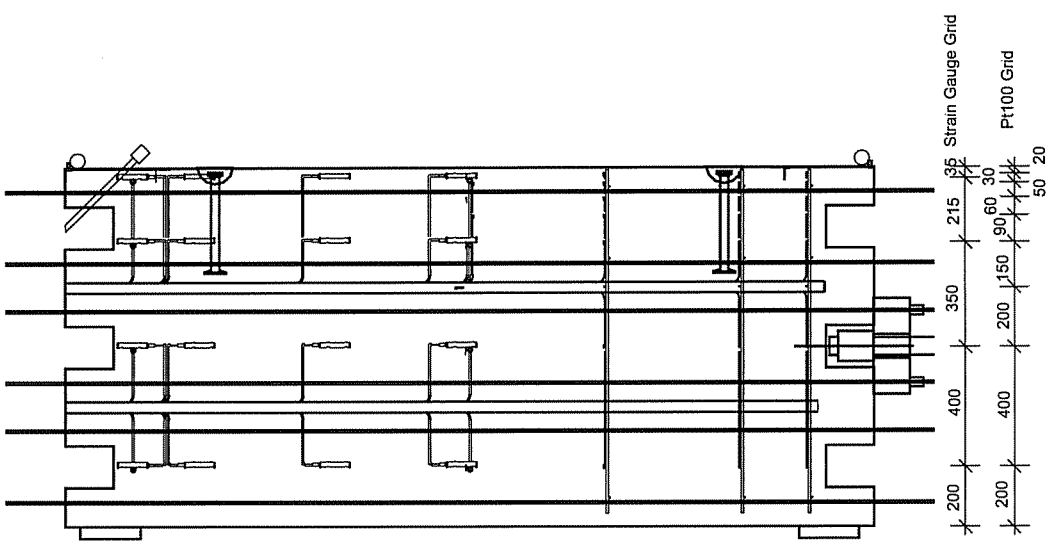

Figure 3: Position of the sensors inside the tested specimen, vertical section (Stegemann, 2005)

The steam test started with the opening of the previously induced cracks to the desired crack width of 0.15 μm at the lower side of the specimen. The crack width at the lower side of the specimen was kept constant during the whole test by adjusting the force in the hydraulick jacks.

Afterwards the pressure and temperature inside the pressure chamber was increased to 0.52 MPa absolute pressure and a temperature of 414.15 K. The mass ratio between steam and air was adjusted to 1.7 and these conditions were kept constant during the 72 hours of the steam test.

3 NUMERICAL INVESTIGATION PERFORMED BY IFMB

For the simulation of the leakage behaviour of reinforced concrete walls, IfMB used a coupled fluid and structure calculation with the finite-element-program ADINA. Two separate models were used: A fluid model and a structural model.

3.1 Description of the Structural Model

To define boundaries for the fluid-structure-interaction (FSI), discrete cracks were used for the structural model. Figure 4 shows the structural model of the specimen. The concrete parts of the specimen were modelled with 4-node solid elements with a 2D-plain stress concrete material model developed at IfMB. For the modelling of the reinforcement, 2-node truss elements were used. The truss elements were connected to the solid elements with 4-node bond elements with an embedded bond model.

According to the experimental set-up the left ends of the reinforcement bars were connected to spring elements. The stiffness of the spring elements was similar to the stiffness of the reinforcement bars with a diameter of 63 mm which were each connected to 4 reinforcement bars lying inside the specimen. The other end of the spring elements was fixed equivalent to the anchorage of the reinforcement bars at the left side of the experimental set-up.

At the right end of the reinforcement bars a force load was applied with the same force on every reinforcement bar as in the experimental set-up. Figure 4 shows the structural model with the applied boundary conditions and loads.

The five inner cracks were equipped with FSI-boundary conditions to allow the interaction with the fluid model. With an iterative calculation the displacements and stresses at these boundaries were coupled between the two models.

3.1.1 Bond elements

There are many different approaches to transfer forces between concrete and reinforcement elements (Akkermann, 2000). In (Keuser, 1985) and (Mainz, 1993) overviews on the different bond element formulations are given. The used formulation of a linear bond element is based on the work of Keuser (1985) and was implemented in ABAQUS by Akkermann (2000). For the calculation of the leakage behaviour it was ported to ADINA.

As element type 4-node isoparametric elements with a linear displacement assumption had been chosen for the implementation of the bond element. In the unloaded state the bond element has only one dimension. It consists of two pairs of nodes. Each pair itself consists of one reinforcement node and one concrete node with the same original position. With nodal displacements the bond element is becoming two-dimensional. Since the nodal displacements are very small compared to the original length of the element, only the line of symmetry between the two node-pairs is considered. This symmetrie line is called contact line (see figure 5). Starting with the global node displacements $\boldsymbol{u}$ of the attached reinforcement and concrete nodes and the help of form functions the local parallel and transversal relative

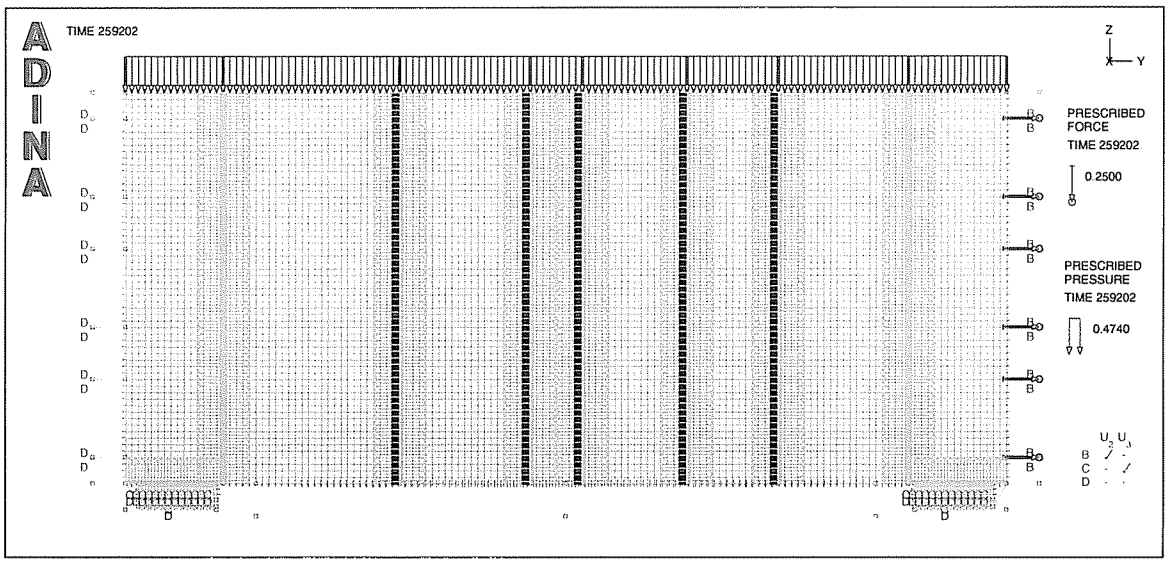

Figure 4: Structural model

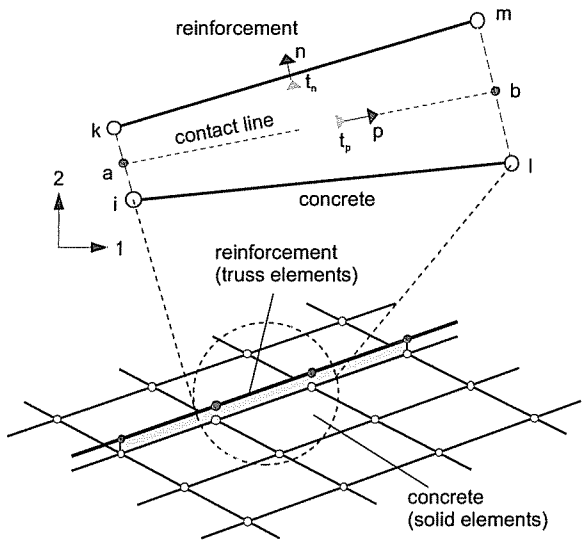

Figure 5: Linear bond element, according to Keuser (1985)

displacements at the contact line were calculated:

$$\delta(p) = \tilde{T} \cdot B \cdot u \tag{1}$$

with

$\tilde{T}$ = transformation matrix from global to local coordinate system,
B = matrix of the form functions.

The stresses $\tau(p)$ at the contact line are then calculated with the local relative slip $\delta(p)$ at the contact line and a bond model. The used bond model is based on the work of den Uijl & Bigaj (1996).

$$\tau(p) = E_b \cdot \delta(p) \tag{2}$$

The component of $\tau(p)$ which is parallel to the reinforcement axis is the bond stress of the bond models. The component perpendicular to the reinforcement axis is the resistance against lateral pressure. With

the stresses and the material stiffness matrix, the nodal force vector and the element stiffness matrix can be calculated (Akkermann, 2000):

$$f_{el} = \frac{l_{el}}{2} \int_{-1}^{1} \boldsymbol{B}^T (\tilde{\boldsymbol{T}}^T \boldsymbol{A}_b \boldsymbol{\tau}) dp, \tag{3}$$

$$\boldsymbol{K}_{el} = \frac{l_{el}}{2} \int_{-1}^{1} \boldsymbol{B}^T (\tilde{\boldsymbol{T}}^T \boldsymbol{A}_b \boldsymbol{E}_b \tilde{\boldsymbol{T}}) dp \tag{4}$$

with

$$\begin{aligned} l_{el} &= \text{element length,} \\ \boldsymbol{A}_b &= \text{contact layer matrix.} \end{aligned}$$

3.1.2 Concrete

In this section a short overview on the used concrete material model will be given. For details, see (Akkermann, 2000).

Concrete is a material with an inhomogeneous structure consisting of coarse aggregates and a continuous matrix, which itself comprises a mixture of cement paste and smaller sand particles (Chen, 1994). Concrete has a highly nonlinear behaviour under mechanical loadings, largely determined by the internal structure of the composite. The deformation behaviour as well as the strength depends on the type of loading. The microscopic material behaviour is determined by a combination of many physical and chemical material laws and implicates many local effects. However, for most of the calculations the global behaviour of the structure is of interest. Macroscopic material models are more suitable for this kind of tasks and the material behaviour is homogenised for this type of material models.

In the implemented material model, a macroscopic damage evolution model (Lemaitre, 1992) is used. In this model, the change of the stiffness of the damaged material depends on the irreversible damage value D:

$$\sigma = (1 - D)\, E_{c0}\, \epsilon, \tag{5}$$

$$D = \text{damage value;} \quad 0 \leq D \leq 1, \tag{6}$$

$$E_{c0} = \text{original stiffness.} \tag{7}$$

The change of the damage value D depends on the load evolution. Since the damage is defined as irreversible, $\dot{D}$ has to be always greater than 0: $\dot{D} \geq 0$. For this reason, the secant stiffness E_{cs}^t is used, if the material is unloaded:

$$E_{cs}^t = (1 - D) E_{c0}. \tag{8}$$

Plastic deformations and time-dependent effects are not considered in the material model that was used.

The material parameters of the concrete and steel were tested at samples by a temperature of 273.15 K. For the material parameters at elevated temperatures (M. Takeuchi *et al.* , 1993) was used. An overview about the used material parameters is given in table 1.

3.2 Fluid Model

The fluid model for the coupled FSI-calculation is shown in figure 6. For the fluid model the following main assumptions have been made:

- Time dependent temperature load on the top surface (pressure chamber)
- Radiation and convection boundaries with a constant environment temperature at the bottom surface

Concrete:	Young's modulus	$E = 31\,400\ \frac{N}{mm^2}$	at 293.15 K
	Young's modulus	$E = 19\,000\ \frac{N}{mm^2}$	at 473.15 K
	Tensile strength	$f_{ct} = 3.0\ \frac{N}{mm^2}$	at 293.15 K
	Compressive strength	$f_{ct} = -57.2\ \frac{N}{mm^2}$	at 293.15 K
Steel:	Young's modulus	$E = 195\,000\ \frac{N}{mm^2}$	
	Yield stress	$E = 552\ \frac{N}{mm^2}$	

Table 1: Material parameters of the structural model

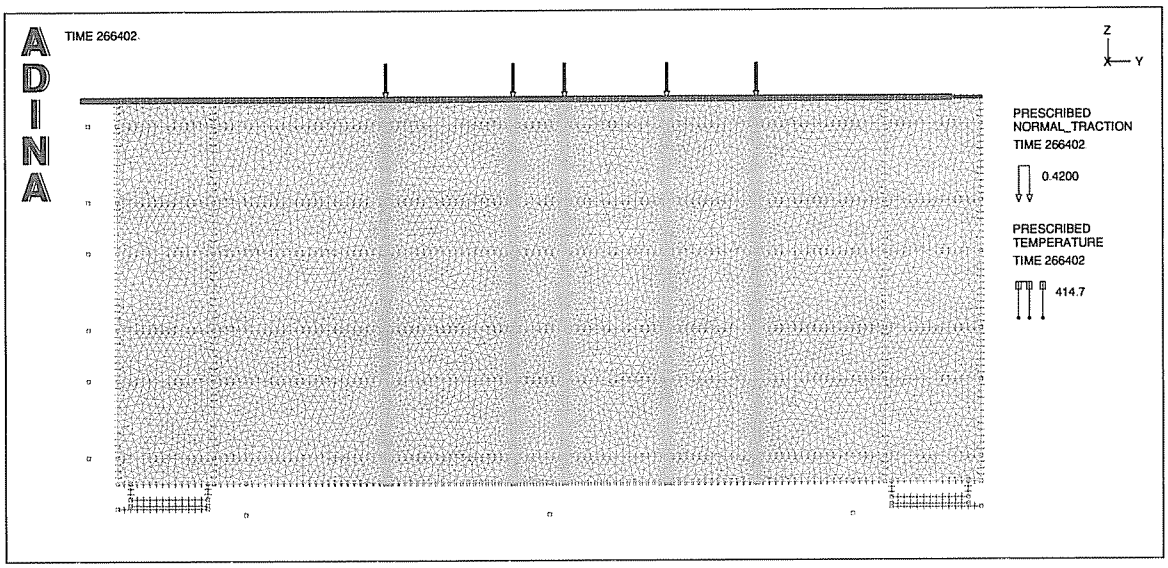

Figure 6: Fluid model

- Constant conductivity and heat capacity of the concrete
- Laminar flow
- Two-Phase flow with the same velocities for the two phases (homogeneous equilibrium model)

The calculated temperatures and pressures at the fluid-structure boundaries of the fluid model were then used as an input parameter for the structural model. The structural model calculates the displacement of the specimen and modifies the fluid-structure boundary of the fluid model for the next iteration step. Table 2 summarises the used material and boundary condition parameters.

3.2.1 Description of the used Laminar Fluid Model

The used Finite Element program ADINA has the possibility to calculate coupled fluid-structure problems. Compared to specialised Computational Fluid Dynamics (CFD) programs like FLUENT, FIDAP, STAR-CD or CFX the capabilities in the fluid part are not as sophisticated as in the specialised CFD programs. On the other hand it is not possible to describe the structural aspects adequately with the CFD programs.

For the description of multiphase fluid flows different models had been developed for example the homogeneous flow model, the separated flow model and the two fluid model (Johnson, 1998). Un-

Concrete:	Thermal Conductivity	$\lambda = 2.3 \frac{kg \cdot m}{s^3 \cdot K}$
	Specific Heat Capacity	$c_p = 1250 \frac{m^2}{s^2 \cdot K}$
Convection:	Convection Coefficient	$H = 8 \frac{W}{m^2 \cdot K}$

Table 2: Thermal material parameters for the fluid model

fortunately ADINA contains no two-phase or multi-phase flow models. Therefore the Homogeneous Equilibrium Model (HEM) is the only possibility to describe the flow conditions inside the cracks of the specimen.

In the homogeneous equilibrium model it is assumed that the velocity, temperature and pressure between the phases or components are equal. This is based on the assumption that differences in these three potential variables will cause momentum, energy and mass transfer between the phases rapidly enough so that equilibrium is reached (Johnson, 1998).

For flows with one phase finely dispersed in another phase like bubbly flow of air in water or steam in water at high pressures this assumption can be made.

The thermodynamic properties of a two-phase flow modelled with the HEM are functions of the volume fractions α_i and the mass fractions X_i of the phase i.:

$$\text{Mixture density} \quad \rho = \sum \alpha_i \cdot \rho_i, \tag{9}$$

$$\text{Internal energy} \quad u = \sum X_i \cdot u_i, \tag{10}$$

$$\text{Specific volume} \quad v = \sum X_i \cdot v_i = \frac{1}{\rho}. \tag{11}$$

Unfortunately the multiphase transport properties of viscosity μ and thermal conductivity k are problematic too, because it is difficult to decide how one should average their effect: in an area average, mass average or volume average sense. For many situations the mixture transport properties have been arbitrarily averaged on a volume average or mass average basis (Johnson, 1998):

$$\mu = \sum \alpha_i \cdot \mu_i \tag{12}$$

or

$$\mu = \sum X_i \cdot \mu_i. \tag{13}$$

Sometimes especially if one phase is dominant like liquid in a channel with low amount of gas the multiphase effects are neglected and the liquid or gas properties of viscosity and thermal conductivity are used.

In our implementation of the homogeneous equilibrium model, the mass average is used for the viscosity, the specific heat and the thermal conductivity of the mixture between the air and the steam/water phase.

The air phase is assumed to be an ideal gas.

3.2.2 Steam Properties

For the pressure and temperature dependent properties of the steam/water phase the IAPWS-IF97 formulation is used (Wagner *et al.* , 1997), (Wagner, 1998).

The IAPWS Industrial Formulation covers the following range:

$$273.15\ K \leq T \leq 1073.15\ K \quad \text{for } p \leq 100\ MPa,$$
$$1073.15\ K \leq T \leq 2273.15\ K \quad \text{for } p \leq 10\ MPa.$$

In the IAPWS-IF97 formulation the properties of water and steam are pressure and temperature dependent and take into account the phase-change between water and steam. In the fluid model the density, viscosity, thermal conductivity and specific heat of the steam/water phase are pressure and temperature dependent.

3.3 Comparison between Calculation and Measurement

For the simulation of the first test with the first specimen, the temperature was applied with a convection boundary condition at the top surface of the specimen. The conductivity and heat capacity of the concrete was kept constant. The measured remaining average crack width of 0.07 mm of the previously opened cracks was taken into account. Crack profiles over the height of the specimen are presented by EDF for different times in figure 17.

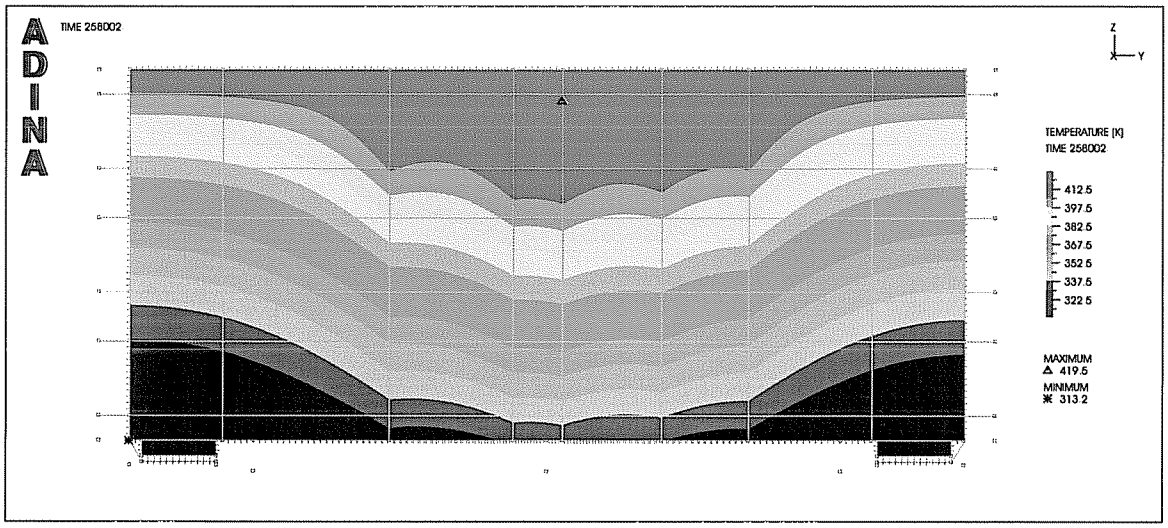

Figure 7: Specimen One: Temperature distribution after 72 h

The fluid is only flowing through the five cracks inside the observation area. The temperature distribution at the end of the calculated steam test (figure 7) shows the influence of the fluid flowing through the cracks on the temperature of the surrounding concrete. Due to the thermal strain of the concrete the displacement and deformation of the specimen is influenced, too.

Figure 8 shows a comparison between the measured and calculated mass flows of air and condensed water. During the first 20 hours the mass ratio of air on the outside of the specimen is lower than the mass ratio of air inside the pressure chamber. Due to the chosen homogeneous equilibrium model the calculated mass ratio between air and steam/water at the outlet side of the specimen is the same as the mass ratio inside the pressure chamber. After 25 hours the calculated water flow is in the same range as the measured one. Unfortunately there were some problems with the measured air flow. Therefore a comparison with the calculated air flow is difficult.

A comparison between the measured and calculated temperatures at different locations inside the specimen in the figures 9, 10 and 11 shows that the calculated temperatures at the top of the specimen near the pressure chamber are too high, especially for the temperature sensors 11 to 18 in the middle of the specimen. The fast increase of the temperatures near the pressure chamber can also be seen in

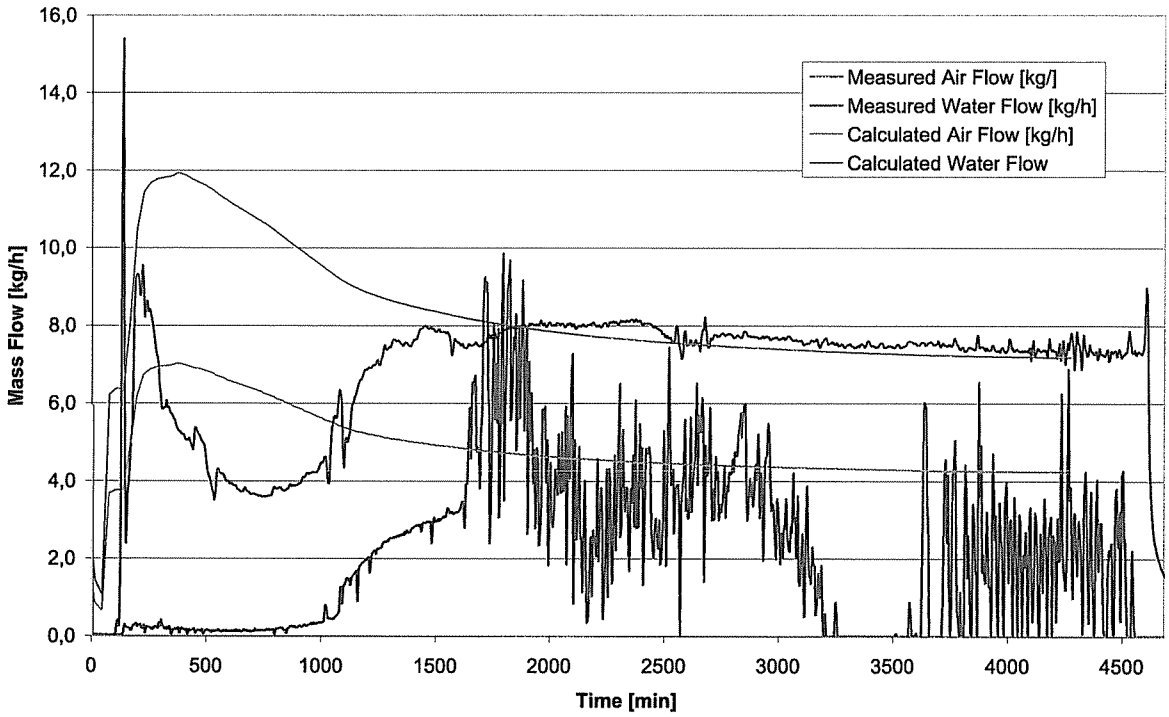

Figure 8: Specimen One: Comparison between measured and calculated leakage flow

the calculation. In the lower part of the specimen the calculated temperatures are underestimated compared to the measured ones. In the future work the parameters for the thermal model have to be improved.

In figure 12 a comparison between measured and calculated strains in the longitudinal direction at different levels at a distance of 0.5 m to the left end of the specimen is given. The peak of the compressive strains at the sensor 31 at the beginning of the experiment is quite the same in the experiment and calculation. Later the calculated compressive strains at this sensor are too high while the calculated compressive strains at the sensor 33 are too low.

A plot of the longitudinal concrete stresses is shown in figure 13. The influence of the bond with the load introduction from the reinforcement into the concrete can be seen in the lower part of the specimen. The concrete stresses at the crack walls are zero and in the middle between the cracks the concrete stresses are at the highest level, because inside the cracks the total force is transfered into the reinforcement bars.

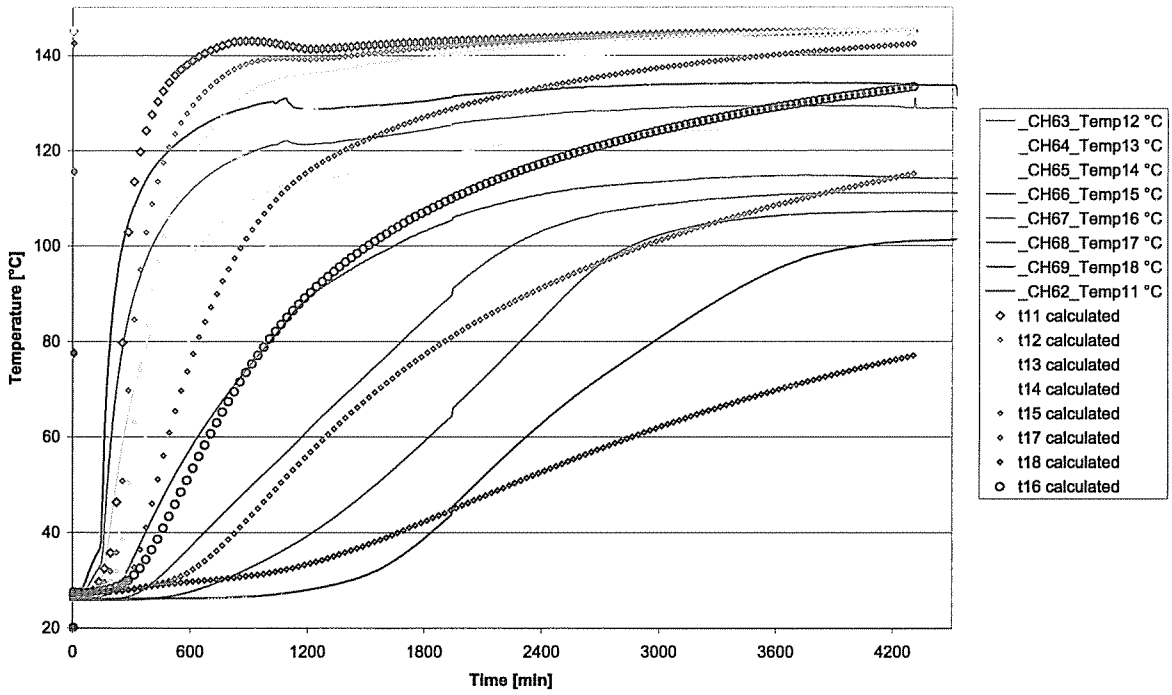

Figure 9: Specimen One: Comparison between measured and calculated temperatures

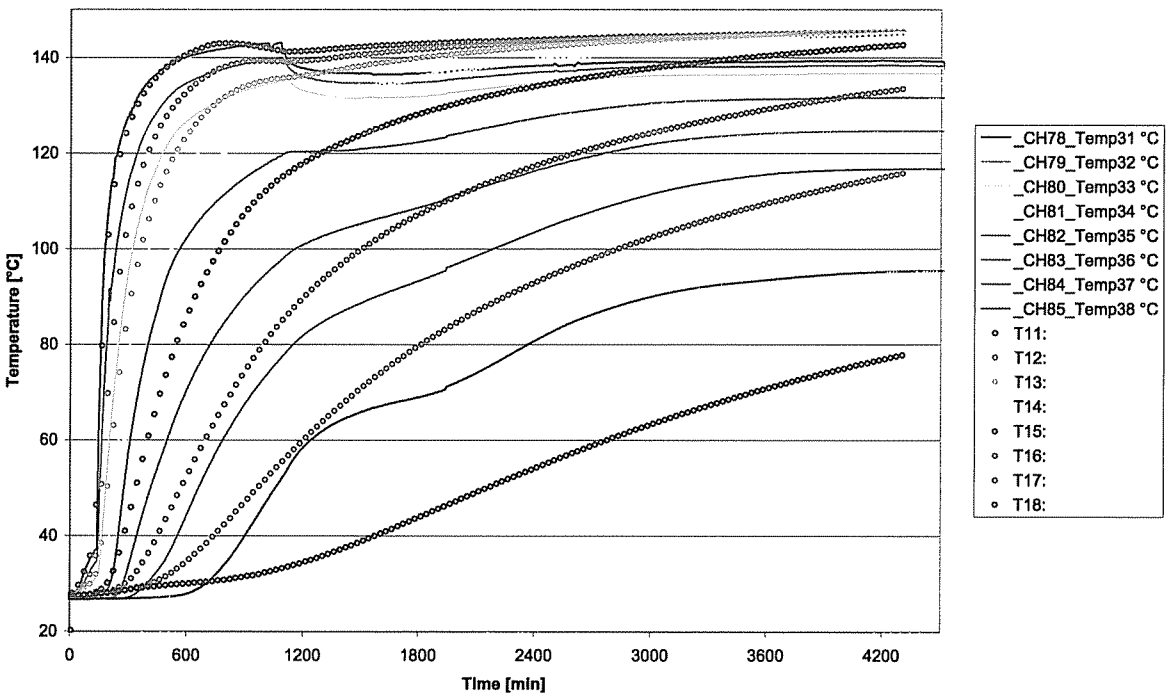

Figure 10: Specimen One: Comparison between measured and calculated temperatures

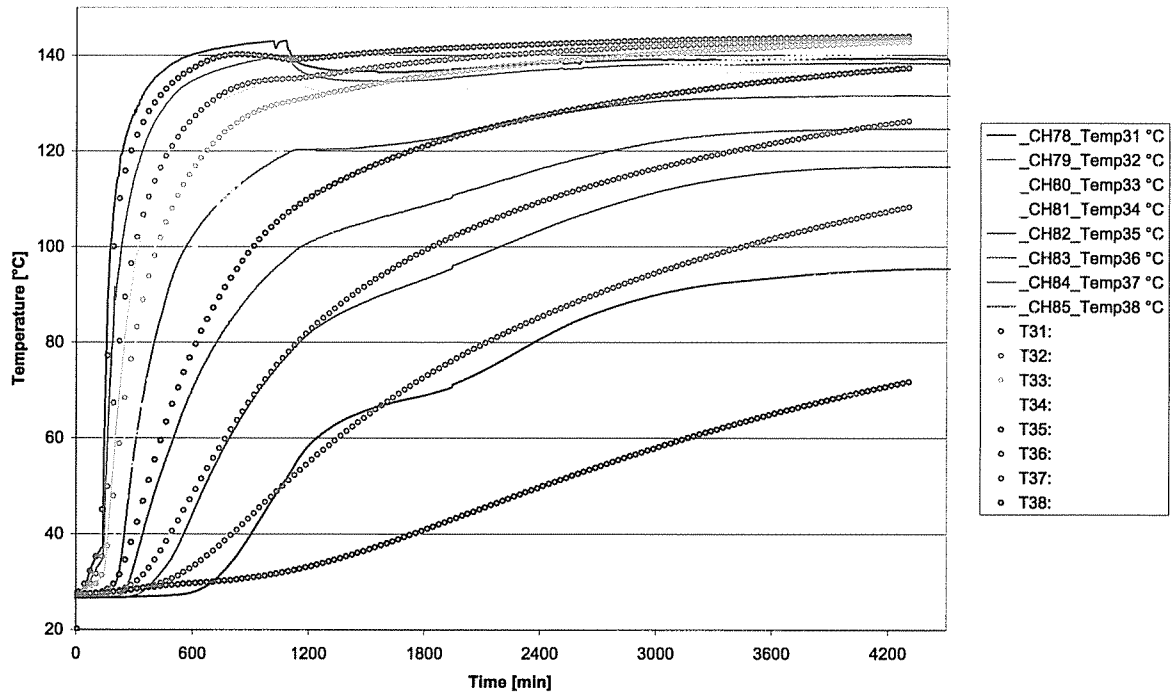

Figure 11: Specimen One: Comparison between measured and calculated temperatures

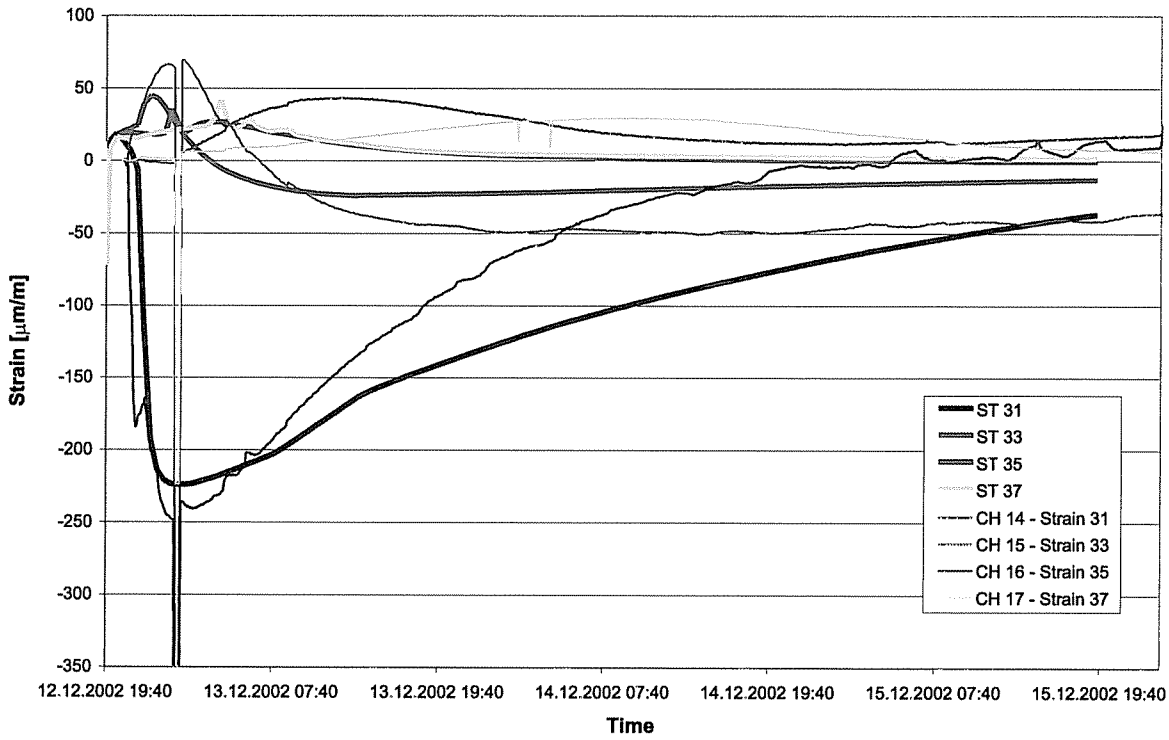

Figure 12: Specimen One: Comparison between measured and calculated strains

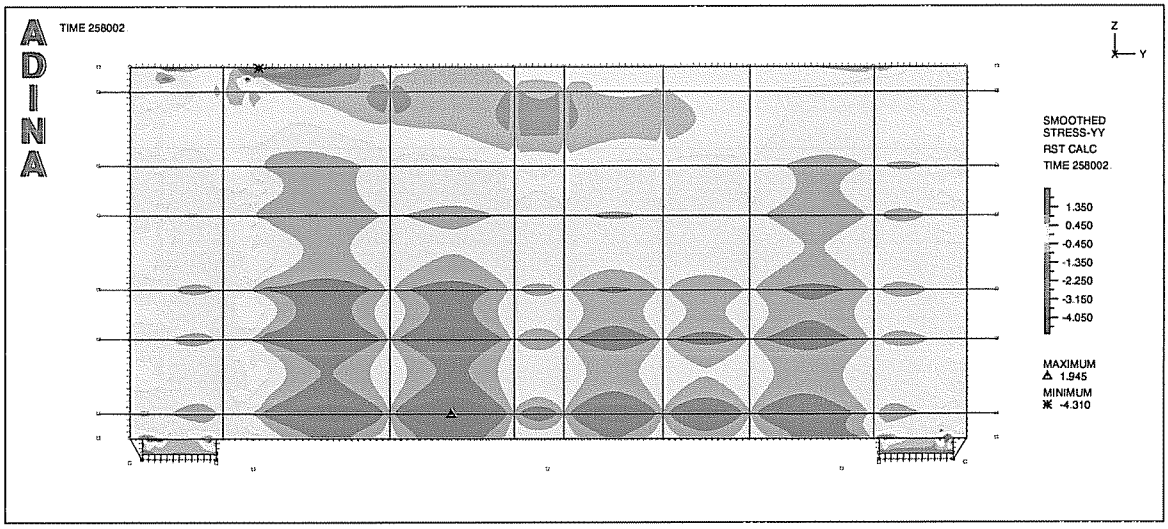

Figure 13: Specimen One: Concrete stresses in longitudinal direction after 72 h

4 NUMERICAL INVESTIGATION PERFORMED BY EDF

The EDF calculation is performed with CODE ASTER® for the thermo mechanics calculations and with ECREVISSE for fluid calculations.

4.1 Principle of the 3D model

One quarter of the slab (symmetry along the main axis, the thickness being conserved to scale 1:1) is represented (length (y) : 1.35 m, width (x) : 0.90 m, depth (z) : 1.20 m). The concrete is modelled with cubic elements. The rebars (length : 1.8 m) are modelled with 1D beam elements. Three discrete cracks are represented, among which two are located in the observation area.The model is shown in figure 14.

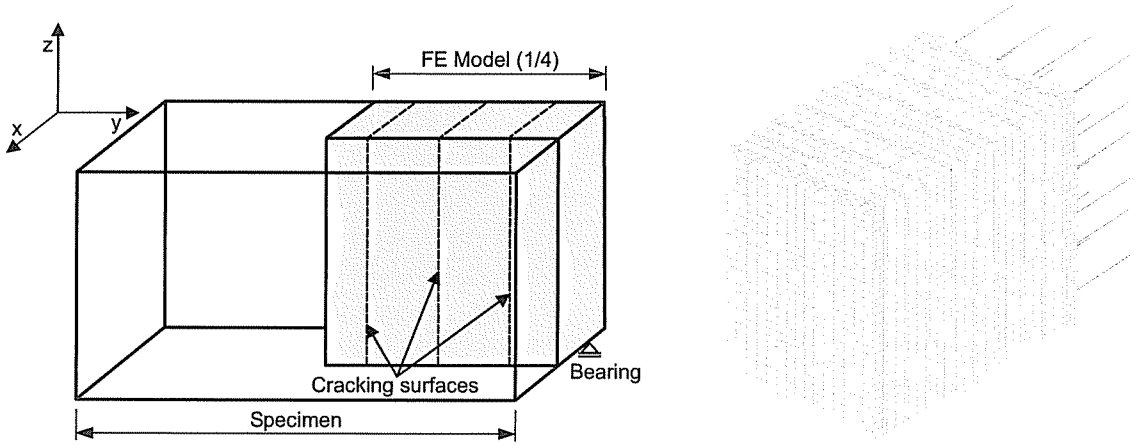

Figure 14: Discrete crack model

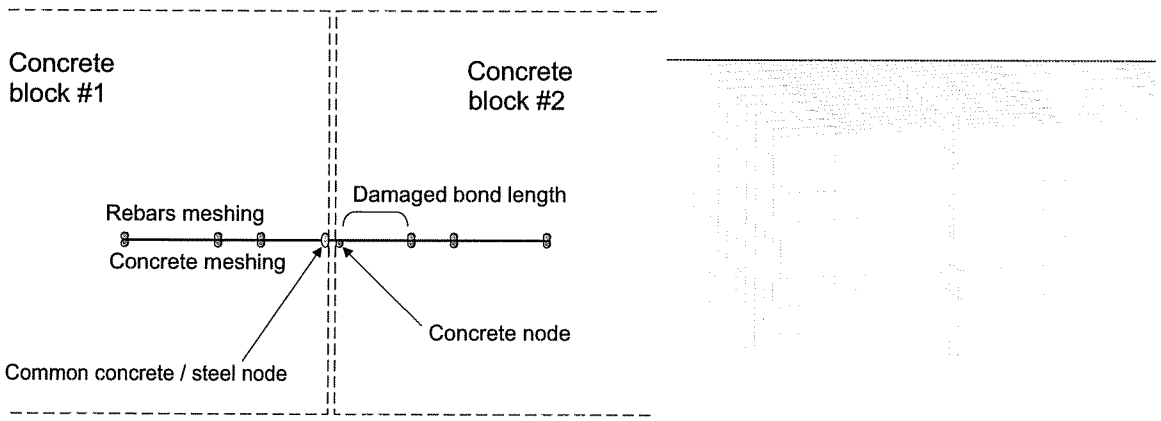

Figure 15: Detail of the discrete crack model

- Among the two concrete nodes located at the crack surface, one belongs to the rebars (fig. 15).
- The crack profile is strongly dependent on the damaged bond length which is simulated by the length of the last rebar element near the crack.
- The vertical displacement of concrete nodes on each block near the rebars must be the same.

The force applied by the hydraulic jacks is taken into account as a displacement at the ends of the rebars.

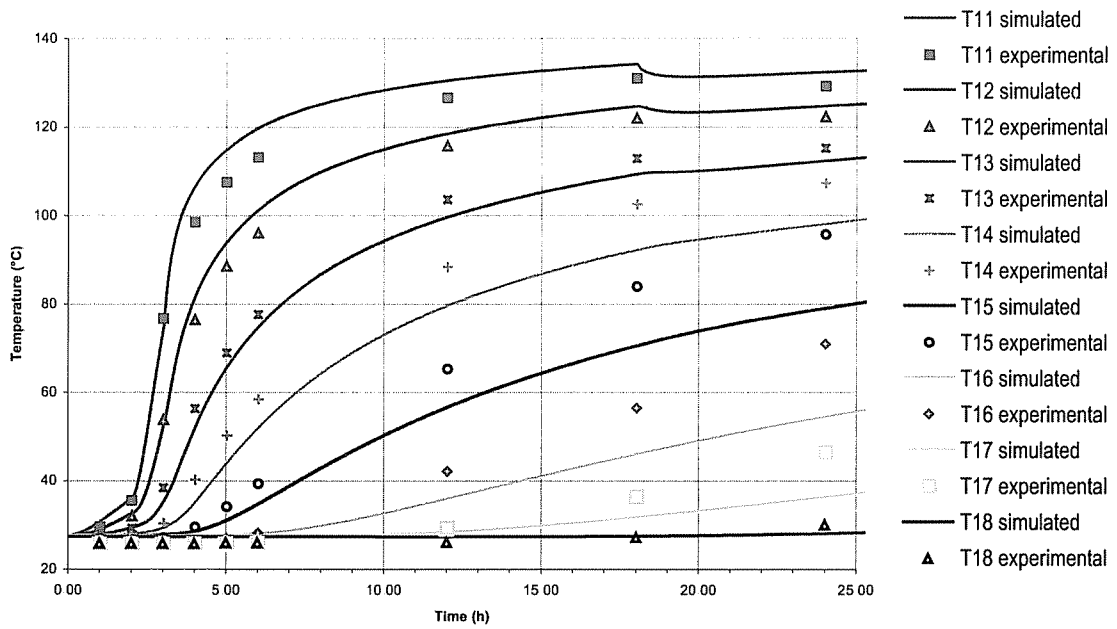

Figure 16: Comparison between measured and calculated temperatures

4.2 Temperature calculation

The temperature is applied at the top surface with a time dependent convection coefficient: 4 $\frac{W}{m^2 \cdot K}$ for the first two hours with a linear increase up to 75 $\frac{W}{m^2 \cdot K}$ during the two following hours. The thermal conductivity is 2.3 $\frac{W}{m \cdot K}$ and the specific heat capacity is 1240 $\frac{J}{kg \cdot K}$.

The calculated temperature values are higher than the experimental results close to the top surface (see figure 16). In the levels between 25 cm and 60 cm below the top surface, experimental temperatures are significantly higher than the calculated ones.

4.3 Thermo mechanics and leakage calculations

4.3.1 Air test

For the calculation, the dead load of the slab, the temperature and the pressure at the top surface are taken into account in order to know the crack profile for the fluid calculation with ECREVISSE.

The first simulation is one of an air test : CODE ASTER® gives crack profiles which are used as input data for leakage calculations with ECREVISSE. Additional required input data is: air, steam and water ratio, pressure and temperature at the top surface. ECREVISSE provides leakage rates and air, steam and water ratio at the bottom surface. As friction and roughness coefficients are adjusted, the model gives good agreement with the experimental results. The main conclusion of the numerical simulation of the air test turns out to be that the best way to represent a closed crack is to model it as an opened crack whose crack width varies from 20 μm to 50 μm. For further air/steam calculations, a value of 40 μm for crack width has been chosen.

4.3.2 Steam test

For the simulation of steam tests CODE ASTER® is used to calculate the crack widths and the temperature of the concrete. Due to the thermal expansion of the concrete the cracks are closing. The calculated crack widths are displayed in figure 17. For the leakage calculation, the minimum crack width is 40 μm,

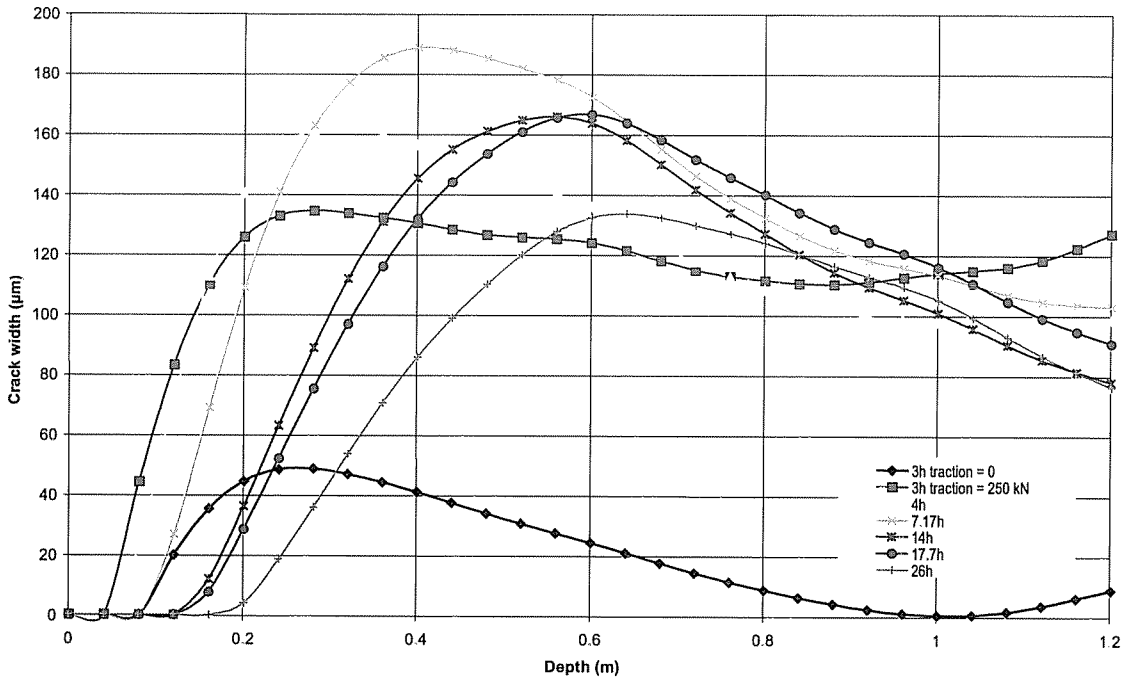

Figure 17: Calculated crack width profiles for several time steps

as explained before.

The calculated crack profiles with an adjustement to a minimum crack width of 40 μm (see figure 18) and calculated temperatures are used as input data for ECREVISSE calculations (1D). The hypotheses for ECREVISSE calculations are that the flow is stationary and the fluid is homogeneous in the perpendicular flow plan. Phase change can occur along the crack: water can vaporise or steam can condense. There is a good agreement in the leakage rate between simulation results and experimental measurements until 14 hours (see fig. 19). After 14 hours, the simulation result slightly decreases although the measurement increase again. The difference is due to the calculated temperatures which are different from the measured ones. But in our model, the temperature dependent dilatation closes the crack and as a result the leakage is reduced.

Other calculations will be performed with the following improvements:

- take into account the fluid structure interaction (effect of fluid pressure and fluid induced heating of the crack walls).
- take into account the fluid pressure in the crack which could widen the crack openings

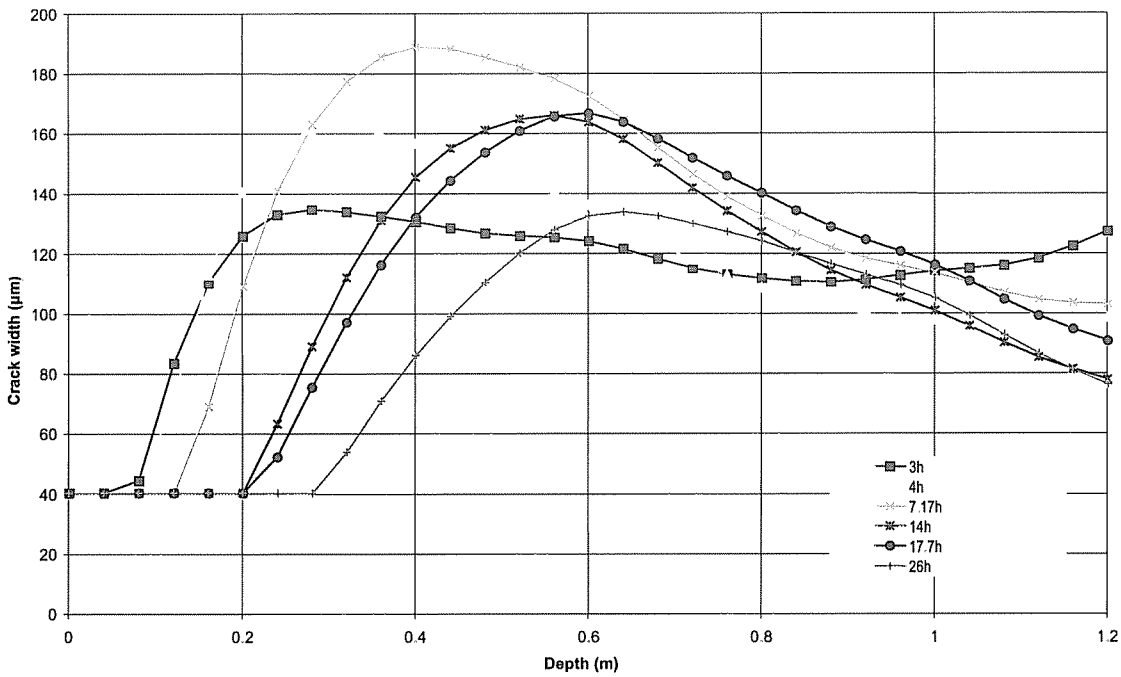

Figure 18: Crack width profiles for leakage calculation with minimum crack width (entry data)

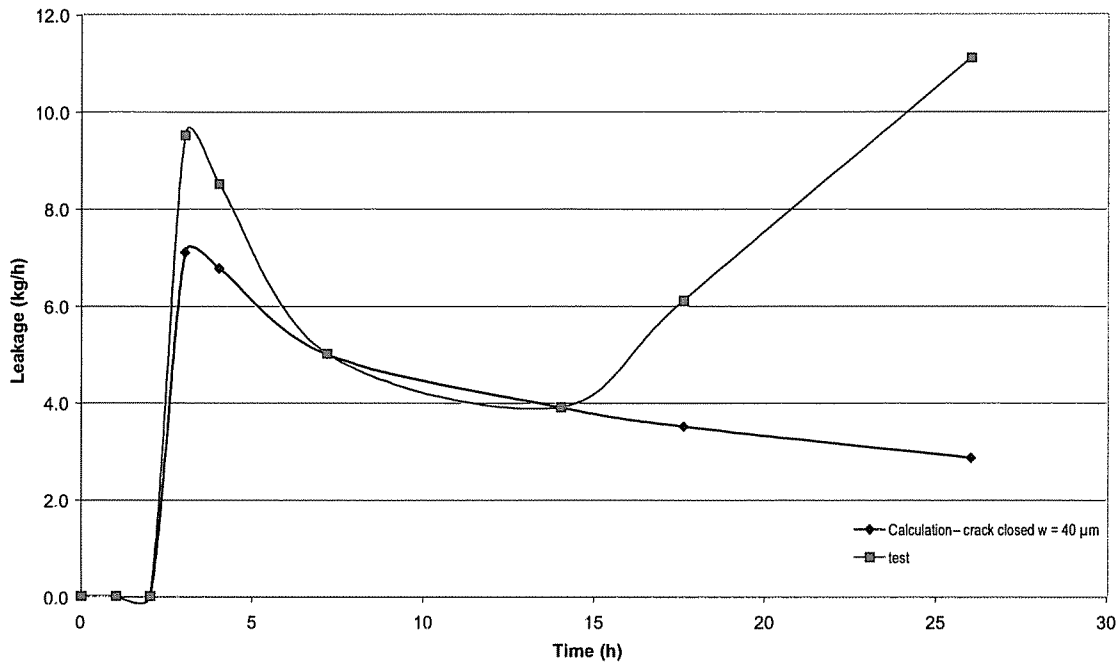

Figure 19: Comparison between leakage calculation and experimental results for water

5 CONCLUSIONS

The leakage behaviour of cracked reinforced concrete walls was investigated experimentally at the Institut für Massivbau und Baustofftechnologie of the Universität Karlsruhe (TH). After a short description of the experimental setup first results of numerical investigations of the leakage behaviour were presented. Two different numerical models were developed at IfMB and EDF.

IfMB used a coupled fluid and structure calculation with the finite-element-program ADINA. Due to the used homogeneous equilibrium model for the calculations of IfMB the velocities of the fluid phases are equal and the mass ratio of the phases remain constant. Therefore the mass ratio at the crack outlet is determined by the mass ratio at the inlet.

In the experiment, especially in the first hours, the mass ratio of air at the outlet side is much lower than the mass ratio of air inside the pressure chamber. With the chosen model the only possibility to simulate this is to change the mass ratio at the inlet side (pressure chamber).

The calculated leakage flow through the five cracks inside the observation area fits the measured leakage flow quite good with the exception of the first few hours of the test and is mainly influenced by the remaining crack width and the mass ratios of the tested air-steam mixture.
EDF used the two programs CODE ASTER® and ECREVISSE for a chained calculation of the experiments. The model of EDF shows a good agreement between the calculation and the measurement for the leakage flow in the first hours. It should be improved within the future work by taking into account the fluid structure interaction.

So far, it has not been considered to model the flow through porous media along the crack in both models.

More investigations should be performed on the temperature behaviour of the specimen due to the following deficiencies:

- In the upper part the calculated temperatures of both models are too high compared to the measured ones especially in the middle of the specimen between the two cracks with the smallest distance. In the IfMB model the concrete is heated too much from the fluid flow inside the cracks.
- In the lower part of the specimen the temperatures are underestimated compared to the measurements.

IfMB and EDF are planning to simulate the tests on the other slabs since the studied one is representative for transgranular cracking which can lead to specific flow rates.

REFERENCES

Akkermann, Jan. 2000. *Rotationsverhalten von Stahlbeton-Rahmenecken.* Ph.D. thesis, Institut für Massivbau und Baustofftechnologie, Universität Karlsruhe (TH).

Caroli, C., Coulon, N., Morton, & Williams. 1995. Theoretical and experimental investigations on the leakage of steam, gas and aerosols through narrow cracks and capillaries. *In: Symposium on EU Research on Severe Accident, Luxembourg.*

Chen, Wai-Fah. 1994. *Constitutive Equations for Engineering Materials.* Elsevier Science B.V.

den Uijl, Joop A., & Bigaj, Agnieszka J. 1996. A bond model for ribbed bars based on concrete confinement. *Heron*, **41**(3), 199–226.

Edvardsen, Carola Katharina. 1996. *Wasserdurchlässigkeit und Selbstheilung von Trennrissen in Beton.* DAfStb 455, Rheinisch-Westfälische Technische Hochschule Aachen.

Greiner, U., & Ramm, W. 1995. Air leakage characteristics in cracked concrete. *Nuclear Engineering and Design*, **156**(1-2), 167–172.

Herrmann, Nico, Niklasch, Christoph, Stegemann, Michael, & Stempniewski, Lothar. 2002 (Apr.). Investigation of the leakage behaviour of reinforced concrete walls. *In: The Evaluation of Defects, Repair Criteria & Methods of Repair for Concrete Structures on Nuclear Power Plants.* OECD Nuclear Energy Agency.

Imhof-Zeitler, Christiane. 1993. *Fließverhalten von Flüssigkeiten in durchgehend gerissenen Betonkonstruktionen.* DAfStb 460.1, Institut für Massivbau, TH Darmstadt.

Johnson, Richard W. (ed). 1998. *The Handbook of Fluid Dynamics.* CRC Press.

Keuser, Manfred. 1985. *Verbundmodelle für nichtlineare Finite-Elemente-Berechnungen von Stahlbetonkonstruktionen.* VDI-Verlag.

Lemaitre, J. 1992. *A Course on Damage Mechanics.* Springer.

M. Takeuchi, M. Hiramoto, N. Kumagai, N. Yamazaki, A. Kodaira, & K. Sugiyama. 1993. Material properties of concrete and steel bars at elevated temperatures. *Pages 133–138 of:* K. Kussmaul (ed), *SMiRT 12*, vol. H.

Mainz, Jürgen. 1993. *Modellierung des Verbundtragverhaltens von Betonrippenstahl.* Ph.D. thesis, Technische Universität München.

Rizkalla, Sami H., Lau, Bon L., & Simmonds, Sidney H. 1984. Air leakage characteristics in reinforced concrete. *Journal of Structural Engineerining*, **110**(5), 1149–1162.

Stegemann, Michael. 2005. *Experimentelle Untersuchungen zur Leckage von Luft- und Dampfgemischen durch gerissene Stahlbetonwände.* to be published in 2005.

Wagner, W., Cooper, J. R., Dittmann, A., Kijima, J., Kretzschmar, H.-J., Kruse, A., Mares, R., Oguchi, K., Sato, H., Stöcker, I., Sifner, O., Takaishi, Y., Tanishita, I., Trübenbach, J., & Willkommen, Th. 1997. *Release on the IAPWS Industrial Formulation 1997 for the Thermodynamic Properties of Water and Steam.* The International Association for the Properties of Water and Steam.

Wagner, Wolfgang. 1998. *Properties of Water and Steam: The Industrial Standard IAPWS-IF97 for the Thermodynamic Properties and Supplementary Equations for other Properties.* Springer-Verlag.